

Improved isotopic model based on ^{15}N tracing and Rayleigh-type isotope fractionation for simulating differential sources of N_2O emissions in a clay grassland soil

Antonio Castellano-Hinojosa^{1,6}, Nadine Loick^{2*}, Elizabeth Dixon², G. Peter Matthews³, Dominika Lewicka-Szczebak⁴, Reinhard Well⁴, Roland Bol⁵, Alice Charteris², Laura Cardenas²

¹Department of Microbiology, Faculty of Pharmacy, University of Granada. Campus Cartuja, 18071-Granada, Spain

²Rothamsted Research, North Wyke, Okehampton, Devon, EX20 2SB, UK

³School of Geography, Earth and Environmental Sciences, University of Plymouth, Davy Building, Drake Circus, Plymouth, PL4 8AA, UK

⁴Thünen Institute of Climate-Smart Agriculture, Bundesallee 65, 38116 Braunschweig, Germany

⁵Agrosphere (IBG-3), Institute of Bio- and Geosciences, Forschungszentrum Jülich, 52428 Jülich, Germany

⁶ Department of Soil Microbiology and Symbiotic Systems, Estación Experimental del Zaidín, 18080-Granada, Spain

* corresponding author: tel: +44 1837 512 300-5279,

e-mail address: Nadine.loick@rothamsted.ac.uk

This article has been accepted for publication and undergone full peer review but has not been through the copyediting, typesetting, pagination and proofreading process which may lead to differences between this version and the Version of Record. Please cite this article as doi: 10.1002/rcm.8374

Abstract

RATIONALE: Isotopic signatures of N₂O can help distinguish between two sources (fertiliser N, or endogenous soil N) of N₂O emissions. The contribution of each source to N₂O emissions after N-application is difficult to determine. Here, isotopologue signatures of emitted N₂O are used in an improved isotopic model based on Rayleigh type equations.

METHODS: The effects of a partial (33% of surface area, treatment 1c) or total (100% of surface area, treatment 3c) dispersal of N and C on gaseous emissions from denitrification were measured in a laboratory incubation system (DENIS) allowing simultaneous measurements of NO, N₂O, N₂ and CO₂ over a 12-day incubation period. To determine the source of N₂O emissions those results were combined with both the isotope ratio mass spectrometry analysis of the isotopocules of emitted N₂O and the ¹⁵N-tracing technique.

RESULTS: The spatial dispersal of N and C significantly affected the quantity, but not the timing of gas fluxes. Cumulative emissions are larger for 3c than 1c. The ¹⁵N-enrichment analysis shows that initially ~70% of the emitted N₂O derived from the applied amendment followed by a constant decrease. The decrease in contribution of the fertiliser N-pool after an initial increase is sooner and larger for 1c. The Rayleigh type model applied to N₂O isotopocules data ($\delta^{15}\text{N}^{\text{bulk}}\text{-N}_2\text{O}$ values) shows poor agreement with the measurements for the original 1-pool model for 1c; the 2-pool models gives better results when using a third order polynomial equation. In contrast, in 3c little difference is observed between the two modelling approaches.

CONCLUSIONS: The importance of N₂O emissions from different N-pools in soil for the interpretation of N₂O isotopocules data was demonstrated using a Rayleigh type model. Earlier statements concerning exponential increase of native soil nitrate pool activity highlighted in previous studies should be replaced with a polynomial increase with dependency on both N-pool sizes.

Keywords:

Greenhouse gas emissions

Denitrification

Isotopes

Isotopocules

Rayleigh type model

Introduction

Agricultural soils rely on external nitrogen (N) inputs and constitute a major source of nitrous oxide (N₂O) and nitric oxide (NO) emissions, accounting for around 10% of greenhouse gas (GHG) emissions from human activities¹ and contributing to the formation of acid rain, eutrophication and ground level ozone². In soil, nitrification and denitrification are the most important microbial processes involved in the production of N₂O, requiring high and low oxygen (O₂) concentrations for the activation of each process, respectively. Moreover, when denitrification occurs, N applied to soils can be emitted back to the atmosphere as dinitrogen (N₂). Many observations have suggested that sequential synthesis of denitrification enzymes is responsible for the delay in N₂ appearance relative to N₂O³⁻⁵.

Amongst the strategies to identify N₂O sources in the soil and their variation in space and time, the study of the natural abundance of stable isotopic signatures of N₂O^{6,7}, such as the $\delta^{15}\text{N}$ and $\delta^{18}\text{O}$ values and the ¹⁵N site preference (SP), have gained attention ever since the early 2000s⁸⁻¹⁰. The N₂O produced from denitrification in soils tends to be associated with $\delta^{15}\text{N}$ signatures with values in the range of -13 to -54‰^{11,12} while those derived from nitrification are up to -60‰^{11,13}. Moreover, reduction of N₂O to N₂ from denitrifying bacteria can be determined by isotopic discrimination as a consequence of the difference in reaction rates of the isotopically light (¹⁴N, ¹⁶O) and heavy (¹⁵N, ¹⁸O) molecules of N₂O¹⁴⁻¹⁶. Interpretation of N₂O isotopomers as indicators of source processes has also been developed^{17,18}. This approach is based on the difference in ¹⁵N occupation of the peripheral (β) and central N-positions (α) of the linear molecule that defines the intra-molecular ¹⁵N SP^{19,20}. The SP is not dependent on the isotopic signature of the precursor²¹, in contrast to average $\delta^{15}\text{N}$ and $\delta^{18}\text{O}$ values of N₂O. However, Sutka et al²² found that the SP is increased during fungal denitrification and nitrification whereas N₂O reduction via denitrification increases the SP by increasing the α -site ¹⁵N-enrichment in the residual N₂O^{9,15}. Wu et al²³ subsequently quantified the potential bias on SP-based N₂O source partitioning using a closed-system model.

Nitrogen fertiliser application to agricultural land can affect the isotopic signature of N₂O and result in two different pools of emissions: pool 1 from fertiliser addition and pool 2 from the native soil N. In addition to those two pools, spatial heterogeneity of denitrification can have a significant impact on N isotope patterns which might only occur in situations where available N and C are added at the same time, e.g. slurry, grazing excreta, urea fertiliser²⁴⁻²⁷. The isotope fractionation during N₂O production^{7,12} and reduction^{15,16}, or when both processes take place simultaneously²⁶, has been previously reported. Moreover, a comprehensive review of isotope effects and isotope modelling approaches was recently presented by Denk et al²⁸. Previously, using a Rayleigh equation to describe isotopic fractionation²⁹, Well and Flessa¹² concluded that the isotopic fingerprint of soil-emitted N₂O is a useful parameter to evaluate the contribution of different processes to the N₂O flux in soils. However, the spatial extent and specific denitrification rates of hypothesized pools could only be constrained by fitting measured and modelled $\delta^{15}\text{N}^{\text{bulk}}$ values, which were associated with considerable uncertainties on the volume and denitrification rates of the assumed pools. Modelling the isotope fractionation during production and reduction based on

the measured temporal pattern of the $\delta^{15}\text{N}^{\text{bulk}}\text{-N}_2\text{O}$ values suggested that there was a multi-pool (non-homogenous) distribution of nitrate (NO_3^-) in the soil ²⁵. Thus, evaluation of isotopologue signatures for identifying source processes was hampered by the simultaneous occurrence of several factors contributing to the time course of isotopic signatures, which could thus not be fully explained. In this sense, Lewicka-Szczebak et al ²⁶ showed that higher denitrification rates resulted in decreasing net isotope effects during N_2O production for ^{15}N using a modelling approach. For N_2O reduction, clearly diverse net isotope effects were observed for the two distinct soil pools. In addition, in a laboratory incubation carried out at different saturation levels for a grassland soil, Cardenas et al ³⁰ found that added N produced higher denitrification rates than soil N, resulting in less isotopic fractionation.

The kinetics of N transformations in soils has been previously explored using an isotopic model based on Rayleigh-type equations ²⁶. This model was developed to simulate $\delta^{15}\text{N}$ values of N_2O using process rates and associated fractionation factors, but assumptions had to be made for some of the model parameters due to a lack of available data. The model is able to evaluate the progress in nitrate consumption and the accompanying isotope effect by fitting the $\delta^{15}\text{N}$ values for the produced N_2O where the $\delta^{15}\text{N}$ values of the residual N_2O are calculated based on the known N_2O reduction ratio. The latter ratio is calculated from direct measurements of the isotopic signature of the remaining unreduced N_2O . The isotopic signature of the instantaneously produced N_2O and the fraction of unreduced N_2O are calculated, based on direct measurements of N_2O and N_2 fluxes. A more comprehensive description of the calculation methods and model construction can be found in Lewicka-Szczebak et al ²⁶. In this context, the aim of the present study was to parameterise the previous 2-pool model via determination of the N_2O production and consumption as well as the N_2O isotopocule signatures of emitted N_2O in a soil treated with a partial and total dispersal of added N and C. The N_2O isotopocule data were used to determine the importance of N_2O emission from different pools using a Rayleigh type model. Controlling the soil volume of pool 1 we assessed the specific denitrification rates of pools 1 and 2 and independently evaluated the contribution of each pool to the total N_2O flux using a parallel ^{15}N tracing experiment. By applying isotopically labelled N, we were able to gain a deeper insight into the proportion of added N that produced the emitted N_2O to estimate the magnitude of pool-derived fluxes.

Materials and Methods

Experimental set up

A clayey pelostagnogley soil of the Hallsworth series (pH in water, 5.6; total N, 0.5%; ammonium N, 6.1 mg kg⁻¹ dry soil; total oxidized N, 15.1 mg kg⁻¹ dry soil; organic matter, 11.7%; clay, 44%; silt, 40%; sand, 15%; w/w) was collected in November 2013 from a typical grassland in SW England, located at Rothamsted Research, North Wyke, UK (50° 46' 50" N, 3° 55' 8" W). Spade-squares (20 × 20 cm to a depth of 15 cm) of soil were taken from 12 locations along a 'W' line across a field of 600 m² size. After collection, the soil was air dried to ~30% gravimetric moisture content, sieved to < 2 mm and stored at 4°C until preparation of the experiment. The experimental design tightly constrained several factors to

study the effects of nutrient concentration and fertiliser application area as previously described²⁷. The soil moisture was adjusted to 85% water filled pore space (WFPS) to promote denitrification conditions, taking the amendment with nutrient solution into account. Before starting the experiment, the soil was preincubated to avoid the pulse of respiration associated with wetting dry soils³¹. For this, the required soil was spread to 3-5 cm thickness. Then, while being mixed continuously, the soil was primed by spraying it with water containing 25 kg N ha⁻¹ of potassium nitrate (KNO₃), which is a typical yearly rate of N deposition through rainfall in the UK^{32,33}. The soil was then left for 3 days at room temperature before being packed into cores and the incubation being started. This was done to promote the growth of denitrifying organisms and prevent a long lag-phase, therefore reducing the length of the experiment.

The incubation experiment was carried out in a specialized gas-flow-soil-core incubation system (DENitrification System (DENIS),³) in which environmental conditions can be tightly controlled. The DENIS simultaneously incubates 12 vessels containing 3 soil cores each (Figure 1). The cores were packed to a bulk density of 0.8 g cm⁻³ to a height of 75 mm into plastic sleeves of 45 mm diameter. The vessels were purged to exclude atmospheric N₂ from the soil and headspace with a He/O₂ mixture (80:20) as described by Loick et al²⁷. The vessels were kept at 20°C during flushing as well as for the 12-day incubation period after amendment application. The experiment was set up to investigate the effect of a heterogeneous distribution of N and C on gaseous emissions from denitrification, by applying the same amount of N and C to each of the three cores within a vessel (100% of total surface area, 3c), or to one of the three cores (33% of total surface area, 1c) (Figure 1). The treatments were physically separated into different cores to remove subsurface lateral dispersion effects and to control the mass transfer coefficient at the surface (see Loick et al²⁷ for further description).

The experiment was carried out with four replicate vessels per treatment (Figure 1): 1c = one of the three cores inside a vessel was amended with KNO₃ and glucose; 3c = all three of the cores inside a vessel were amended with KNO₃ and glucose; Control = only water was applied to each of the three cores. Within each of the 1c and 3c treatments two of the four vessels received ¹⁵N-labelled KNO₃ (5 at%). The experiment was carried out twice, resulting in four labelled and four unlabelled replicates per treatment. Considering the total surface area of the vessel (sum of the areas of the three cores in a vessel), N was applied at a rate of 75 kg N ha⁻¹ and C as glucose at 400 kg C ha⁻¹ for treatment 3c where N and C were diluted in 15 mL water and 5 mL of that solution was added to each of the three cores inside one vessel. For treatment 1c, N was applied at a rate of 25 kg N ha⁻¹ and C as glucose at 133.3 kg C ha⁻¹, being applied in solution with 5 mL water to one of the three cores, while the other two cores each received 5 mL water only. The amendment was applied to each of the three cores via a syringe through a sealed port on the lid of the incubation vessel.

Gas analyses and data management

The gas emissions were measured every 10 min consecutively in vessels 1 to 12, resulting in bi-hourly measurements for each vessel. The fluxes of N₂O, CO₂ and N₂ were quantified by

gas chromatography using an electron capture detector (ECD) for N₂O, and a helium ionization detector (HID) for CO₂ and N₂, respectively, while the NO concentrations were determined by chemiluminescence, as described by Loick et al ²⁷. The flow rates through the vessel were measured daily and used to correct all gas concentrations and convert them to flux units (kg N or C ha⁻¹ d⁻¹). The CO₂ fluxes showed constant emissions of 0.67 kg C ha⁻¹ h⁻¹ before and after the peak in all vessels, which we consider to be a baseline flux. In order to show emissions attributed to amendment application only, the CO₂ fluxes in all the treated vessels were adjusted by subtracting this baseline. The initial emission rates for each gas and vessel were determined from the beginning of each peak until the increase in concentrations slowed down, as previously described by Loick et al ²⁷.

Analysis of the isotopocules of N₂O

Gas samples for isotopocule analysis of the emitted N₂O were taken 4 hours after amendment application and then daily from unlabelled and control treatments. Samples were collected in two 115-mL septum-capped serum bottles, which were connected in line to the vent of each vessel. The isotopocule signatures of N₂O, i.e. δ¹⁸O (δ¹⁸O-N₂O) values, average δ¹⁵N (δ¹⁵N^{bulk}-N₂O) values and δ¹⁵N values from the central N-position (δ¹⁵N^α), were determined by isotope ratio mass spectrometry ⁷. The ¹⁵N site preference (SP) was obtained as SP= 2 * (δ¹⁵N^α - δ¹⁵N^{bulk}-N₂O). The isotopocule ratios of a sample were expressed as ‰ deviation from the ¹⁵N/¹⁴N and ¹⁸O/¹⁶O ratios of the reference standard materials, atmospheric N₂ and standard mean ocean water, respectively, as described by Bergstermann et al ²⁵.

Isotopic analysis of N₂O in ¹⁵N-labelled treatments

Gas samples for ¹⁵N analysis were taken just before (0 h) and 4 h after amendment application and then daily for the first week, followed by a final sampling at day 11. The sampling dates were chosen to cover changes in isotopic ratios during the main period of NO and N₂O fluxes, and after the emissions returned to background levels. Samples were taken from the outlet line of each vessel using 12-mL exetainers (Labco, Lampeter, UK) which had previously been flushed with He and evacuated. The ¹⁵N-enrichment of N₂O was determined using a TG2 trace gas analyser (Sercon, Crewe, UK) and a Gilson autosampler (Gilson, Dunstable, UK), interfaced to a Sercon 20-22 isotope ratio mass spectrometer. Standard solutions of 6.6 and 2.9 at% ammonium sulphate ((NH₄)₂SO₄) were prepared and used to generate samples of 6.6 and 2.9 at% N₂O ³⁴ which were used as reference and quality control standards. The ¹⁵N content of the N₂O was calculated as described by Loick et al ²⁷ to determine how much of the measured N₂O derived from the NO₃⁻ amendment rather than the native soil N.

Soil analyses

The moisture contents and NH₄⁺ and NO₃⁻ concentrations were determined in soil samples taken at the beginning and end of the incubation. At the end of the soil incubation time, each core was divided in half to separate the top section from the bottom section. The WFPS was calculated from the soil moisture contents by drying a subsample (50 g) at 105°C overnight.

The soil NH_4^+ -N and NO_3^- -N were measured by automated colorimetry from 2 M KCl soil extracts using a Skalar SANPLUS Analyser (Skalar Analytical B.V., Breda, The Netherlands) ³⁵.

Model refinement

A comparison of modelled and measured data for the previously used Rayleigh model ²⁶ and the Rayleigh model adapted to the N_2O isotopocule data (determined in this study) was applied to account for isotope effects associated with N_2O reduction, taking emissions from two distinct soil pools (NO_3^- added with the amendment = pool 1; native soil NO_3^- = pool 2) into account. The previous used Rayleigh model ²⁶ assumes an exponential increase in the N_2O originating from pool 2 after amendment application until nitrate in pool 1 is exhausted. However, this exponential increase was only an assumption and not experimentally confirmed. Hence, we used the ^{15}N -labelled treatments to determine the equation that best describes the mixing dynamics of the two NO_3^- pools. The Rayleigh model was then run with the isotopocule data from the unlabelled treatments, but using the equation determined before using the ^{15}N labelled treatments. In this study, the volume reached by the amendment (volume of pool 1) was assumed to be 33% and 100% in 1c and 3c treatments, respectively. For modelling, we applied the equations described in Lewicka-Szczebak et al ²⁶. Briefly, the isotopic signature of the product, N_2O and the isotopic signature of the remaining substrate, NO_3^- , was calculated according to Eqn. 1:

$$\frac{\delta_S - 1000}{\delta_{S0} - 1000} = f^{\frac{\eta_{p-s}}{1000}} \quad (1)$$

where δ_S is the isotopic signature of the remaining NO_3^- ($\delta^{15}\text{N}_{\text{NO}_3\text{-r}}$); δ_{S0} the isotopic signature of the initial NO_3^- ($\delta^{15}\text{N}_{\text{NO}_3\text{-i}}$), i.e., fertiliser or soil NO_3^- ; and η_{p-s} the Net Isotope Effect (NIE) between product and substrate.

In this study, we determined the $\delta^{15}\text{N}$ value of the applied fertiliser whereas that of soil NO_3^- was adapted from the literature ²⁶:

$\delta^{15}\text{N}_{\text{soil NO}_3^-} = 10\text{‰}$. f , the fraction of unreduced NO_3^- -N, was determined by subtracting the initial NO_3^- concentration and the cumulative N loss as denitrification products ($\text{N}_2 + \text{N}_2\text{O}$) for each time step of the process:

$$f = (\text{N}_{\text{NO}_3\text{-i}} - \text{N}_{\text{N}_2 + \text{N}_2\text{O}}) / \text{N}_{\text{NO}_3\text{-r}} \quad (2)$$

It was assumed that the NO and NO_2^- pools were negligible in the overall N balance, as these represent very reactive intermediate products undergoing fast further reduction. η_{p-s} represents the Net Isotope Effect (NIE) of N_2O production referred to as $\eta_{\text{N}_2\text{O}-\text{NO}_3}$. The $\delta^{15}\text{N}_{\text{N}_2\text{O-p}}$ (instantaneously produced N_2O) value was calculated according to Eqn. 3:

$$\delta^{15}\text{N}_{\text{N}_2\text{O-p}} \cong \delta^{15}\text{N}_{\text{NO}_3\text{-r}} + \eta^{15}\text{N}_{\text{N}_2\text{O}-\text{NO}_3} \quad (3)$$

The isotopic signature of the reduced N_2O was calculated according to Eqn. 1, where δ_S is the isotopic signature of the remaining unreduced N_2O ($\delta_{\text{N}_2\text{O-r}}$); δ_{S0} the isotopic signature of the instantaneously produced N_2O ($\delta_{\text{N}_2\text{O-p}}$); f the fraction of unreduced N_2O , calculated based on direct measurements of the N_2O and N_2 flux, i.e., the product ratio ($\text{N}_2\text{O}/(\text{N}_2\text{O} + \text{N}_2)$); and η_{p-s} is the NIE of N_2O reduction referred to as $\eta_{\text{N}_2-\text{N}_2\text{O}}$.

Statistical analysis

Data were analysed to determine normality (Kolmogorov-Smirnov test) and equality of variance (Levene test) conditions. To fulfil these assumptions, the data were log-transformed before analysis, if needed. Statistical analysis was performed using GenStat 16th edition (VSN International Ltd, Hemel Hempstead, UK). Cumulative emissions were calculated after linear interpolation of the area between sampling points. Differences in total emissions between treatments for each gas measured were assessed by ANOVA at $p < 0.01$.

Results

Fluxes and cumulative gas emissions

The fluxes and cumulative emissions of NO, N₂O, N₂ as kg N ha⁻¹ and CO₂ are shown in Figure 2 and Table 2, respectively. The NO emissions from the 1c and 3c treatments increased immediately after amendment application with a peak lasting just over 2 days and a maximum on day 1 (Figure 2). The mean cumulative NO emissions from the 3c (same shape) treatment was about 2.3 times greater over the time of the incubation than that from the 1c treatment (Table 2). Emissions of NO from the Control treatment were negligible.

Similarly to the observed NO emissions, the N₂O emissions increased immediately after amendment application (Figure 2). The emissions from the 3c treatment peaked 3.5 days after the amendment was applied, before decreasing again. The maximum N₂O emission was larger for the 3c treatment than for the 1c treatment. In the 1c treatment, however, there was a plateau in N₂O emissions from about day 2 to day 4 before showing the same decrease as the 3c treatment. The cumulative emissions of N₂O (Table 2) were 2.9 times greater from the 3c treatment than from the 1c treatment. The Control treatment only showed very small N₂O emissions from 1 to 2.5 days after water addition.

The N₂ fluxes increased after amendment application in the 1c and 3c treatments and water addition in Control treatment (Figure 2). Slightly higher N₂ fluxes were measured in the 3c treatment than in the 1c and Control treatments, showing a peak after 2 days in the 3c treatment (Figure 2). In contrast to the NO and N₂O emissions, the N₂ cumulative emissions were similar for the 1c and Control treatments, whereas significant higher N₂ cumulative emissions were measured in the 3c treatment (Table 2).

The total denitrification was calculated as the sum of all the N emitted (Table 2) and was significantly higher in the 3c treatment than in the 1c (2.8-fold) and Control (6.1-fold) treatments.

The CO₂ fluxes showed similar trends to the N₂O fluxes. In the 1c and 3c treatments, the CO₂ emissions increased immediately after amendment application (Figure 2) and peaked after about 3 days in both treatments. The cumulative emissions of CO₂ (Table 2) were 1.6 and 2.6 times greater from the 3c treatment than from the 1c and Control treatments, respectively. CO₂ emissions above background levels were negligible for the Control treatment.

Soil mineral N

The results of the soil analysis at the end of the incubation are given in Table 1. The NO₃⁻ concentrations were significantly different between the top and the bottom half of the cores

for the amended treatments but no significant difference was detected within the Control treatment. The results, if considering the whole vessel, did, however, show that there was a significant difference in the NO_3^- concentrations between the 1c and 3c treatments in the top layer ($p < 0.05$). Both amended treatments showed significantly higher NO_3^- concentrations than those in the Control treatment.

Regardless of the treatment, the NH_4^+ concentrations were lower than the NO_3^- concentrations at the end of the incubation, with significantly higher values in the bottom layer of the core. Both soil NH_4^+ and NO_3^- increased in all treatments compared with the initial soil conditions (6.1 and 15 mg N kg dry soil⁻¹). The NH_4^+ concentrations were only significantly different between treatments in the top layer, in decreasing order: Control > 1c > 3c. The soil moisture content was significantly different between the top (83.2 ± 0.50) and the bottom (76.0 ± 0.56) half of the cores at the end of the incubation in all treatments.

¹⁵N-enrichment of N₂O in the ¹⁵N-labelled treatment

The ¹⁵N-enrichment of the emitted N₂O is shown in Figure 3. Regardless of the N treatment, up to day 4 around 70% of the emitted N₂O was derived from the applied amendment, with a constant decrease thereafter (Figure 3). After 4 days, when N₂O emissions decrease while the N₂ fluxes increase (Fig. 4), which indicates that N₂O reduction dominates over N₂O production, the enrichment in ¹⁵N of the N₂O decreases. This decrease is faster in the 1c treatment than in treatment 3c, reaching a final contribution of fertiliser N to N₂O emissions of around 20% and 50%, respectively, by day 11.

Isotopic signature of N₂O in the non-labelled treatments

$\delta^{15}\text{N}^{\text{bulk}}$ values of N₂O

The $\delta^{15}\text{N}^{\text{bulk}}$ -N₂O values were not significantly different between the N-amended treatments during the first 4 days, and increased from an initial value of about -23.4‰ in both treatments to -1.1‰ and -5.5‰ in the 1c and 3c treatments, respectively (Table 3). After 4 days, the $\delta^{15}\text{N}^{\text{bulk}}$ -N₂O values remained relatively constant in the 3c treatment, in the range of -1.2-1.7‰, until the end of the incubation. In contrast, in the 1c treatment the $\delta^{15}\text{N}^{\text{bulk}}$ -N₂O values increased until day 6 (10.4‰) and declined by day 9 (-4.2‰), peaking again on day 11 (51.8‰). Immediately after water addition, the $\delta^{15}\text{N}^{\text{bulk}}$ -N₂O value of the Control treatment was -23.8‰ and it peaked on day 6 (10.4‰) to decrease afterwards until -20.7‰ on day 11 (Table 3).

¹⁵N site preference of N₂O

The ¹⁵N site preference of N₂O (SP-N₂O) of both N-amended treatments decreased slightly for the first 4 days and gradually increased thereafter until the end of the incubation, showing only small differences between them (Table 3). Overall, the SP N₂O values increased from an initial value in the range of -1.6 and -4.9‰ to a maximum of approximately 9.4‰ and 4.3‰ in the 1c and 3c treatments, respectively (day 11 after application). The SP N₂O from the Control treatment increased after the application of water up to 22.5‰ and declined to -4.1‰ by day 2, increasing gradually until the end of the incubation to reach a final value of 22.9‰

(Table 3). The $\delta^{15}\text{N}^{\alpha}$ and $\delta^{15}\text{N}^{\beta}$ values followed a similar trend to the $\delta^{15}\text{N}^{\text{bulk}}$ values with small differences between the isotope ratios, and generally $\delta^{15}\text{N}^{\alpha} > \delta^{15}\text{N}^{\beta}$ (data not shown).

$\delta^{18}\text{O}$ values of N_2O

Similar to the N_2O SP, the $\delta^{18}\text{O}$ values of N_2O showed small differences in the temporal pattern between the 1c and 3c treatments (Table 3). Overall, the $\delta^{18}\text{O}$ values of the N_2O in both N-amended treatments increased continuously from an average 29.4‰ to 40.4‰ at the end of the incubation. In the Control treatment, the $\delta^{18}\text{O}$ values of N_2O increased after water application to 39.7‰, followed by a decline to 18.9‰ by day 2. Afterwards, the value gradually increased until the end of the incubation to about 37.6‰ (Table 3).

An X/Y plot of $\delta^{18}\text{O}-\text{N}_2\text{O}$ values against $\delta^{15}\text{N}^{\text{bulk}}-\text{N}_2\text{O}$ values is presented in Figure 4. Regardless of the treatment, both isotope ratios increased at a ratio of approximately 1:3 during the incubation. A similar behaviour was observed in both N-amended treatments, which indicated that the ratio of the simultaneous increase in the $\delta^{18}\text{O}-\text{N}_2\text{O}$ and $\delta^{15}\text{N}^{\text{bulk}}-\text{N}_2\text{O}$ values did not differ between treatments (Figure 4). Moreover, the $\delta^{18}\text{O}-\text{N}_2\text{O}$ and $\delta^{15}\text{N}^{\text{bulk}}-\text{N}_2\text{O}$ values grouped into two separate clusters depending on whether they were measured from samples taken before or after the N_2O peak. As expected, a different trajectory in the $\delta^{15}\text{N}^{\text{bulk}}-\text{N}_2\text{O}$ and $\delta^{18}\text{O}-\text{N}_2\text{O}$ values was observed in the Control treatment over the experimental period.

The X/Y plot of $\delta^{18}\text{O}-\text{N}_2\text{O}$ values against SP in Figure 5 shows the “map” for the values of $\delta^{18}\text{O}$ and SP from all unlabelled treatments. Reduction lines (vectors) represent minimum and maximum routes of isotopocule values with increasing N_2O reduction to N_2 based on the reported range in the ratio between the isotope fractionation factors of N_2O reduction for SP and the $\delta^{18}\text{O}$ values¹⁸. Most of the values measured after amendment application, but before the N_2O peak are below the lower reduction line, but within the area indicating bacterial denitrification. During the N_2O peak the samples show increased $\delta^{18}\text{O}$ values followed by an increased SP after the peak.

Modelling ^{15}N -enrichment of N_2O

Measurements of ^{15}N -enrichment using the 1c- and 3c ^{15}N -labelled treatments (Figure 3) derived in the polynomial Eqn. 4 and Eqn. 5, respectively, were:

$$f(x) = 0.1488 x^3 - 2.9435 x^2 + 10.892 x + 55.28; R^2=0.8532 \quad (4)$$

$$f(x) = 0.092 x^3 - 1.8938 x^2 + 8.5897 x + 59.56; R^2=0.8514 \quad (5)$$

where $f(X)$ is the contribution of fertiliser N to N_2O in % and x is the time after amendment (d).

The Rayleigh model fit adapted to ^{15}N data for the 1c and 3c unlabelled treatments was evaluated in all vessels, assuming 1-pool and 2-pool emissions. Only two vessels per treatment ($n=4$) showed a good polynomial fit ($R^2 > 0.89$) of the modelled data to the measured data and an average of them is shown in Figure 6. The equations and R^2 values of all the vessels for each N pool are shown in Table S1 (supporting information). The Rayleigh model applied to the $\delta^{15}\text{N}^{\text{bulk}}-\text{N}_2\text{O}$ data showed poor agreement with the measurements using the original model for 1c treatment, with the 2-pool model giving better results when using

the polynomial equation determined above (Figure 6). In contrast, for the 3c treatment little difference was observed between the modelling approaches (Figure 6).

Discussion

Soil data and gaseous emissions

Our findings are in agreement with those found by Wang et al.³⁷ and Loick et al.²⁷, which found that the emission of NO, N₂O and CO₂ is related to the amount of applied NO₃⁻ and C, NO₃⁻ and C thereby being the limiting factors for denitrification activity, rather than the soil area and volume and associated microbial population that receives the amendment. Although the total emissions were not similar, the peak of N₂O, NO and CO₂ fluxes were concurrent in the 1c and 3c treatments. Moreover, the amendment solution was spread over all three cores in the 3c treatment which could have potentially supported a three times larger microbial community with the nutrients than the 1c treatment. Loick et al.²⁷ found a delay in the N₂O emission peak when only one of three cores inside a vessel was amended with the full amount of nutrients, compared with an equal distribution of the treatment into three cores (so each core received 1/3 of the nutrients). In our case, in the 1c and 3c treatments all individual cores (one in 1c and three in 3c) received the same amount of nutrients and the response time was similar, showing that denitrifiers transformed the NO₃⁻ added to N₂O for the same time period in both treatments, regardless of the soil area/volume amended. Although the cumulative emissions of N₂ were higher in the 3c treatment, the fluxes were lower than N₂O fluxes in all treatments. It has been demonstrated that many denitrifiers lack one or more of the denitrification enzymes involved in all reduction steps from NO₃⁻ to N₂³⁸, particularly N₂O reductase (NosZ) the enzyme reducing N₂O to N₂. In addition, the last step in denitrification is also the least energetically favourable³⁹. Therefore, denitrifiers would preferentially reduce NO₃⁻ to N₂O rather than N₂O to N₂. We hypothesized that these reasons explain the accumulation of N₂O over N₂^{27,40}.

Isotope analysis of N₂O from ¹⁵N-labelled treatments

The ¹⁵N signature of N₂O was used to determine the contribution of the native soil NO₃⁻ or the NO₃⁻ added with the amendment to the N₂O emissions (Fig. 3). While in the 3c treatment N₂O emissions were mainly from the added NO₃⁻ (pool 1) throughout the whole experimental period, in the 1c treatment, a low ¹⁵N enrichment of the measured N₂O was observed after 5 days, indicating that after this time most of the emitted N₂O was from the native soil NO₃⁻ (pool 2). This can be explained due to NO₃⁻ limitation in the soil treated in the 1c treatment after the N₂O peak. Because only one third of the soil/microbial community received nutrient amendment, N₂O emissions were low in the 1c treatment and those from the non-amended cores are likely to mask the effect of the amendment on N₂O production²⁷. Moreover, after 11 days, N₂O production in the 3c treatment still came from the NO₃⁻ added.

Isotopocules analysis of N₂O

$\delta^{15}\text{N}^{\text{bulk}}$ -N₂O values

The increase in $\delta^{15}\text{N}^{\text{bulk}}$ -N₂O values until day 4 in both 1c and 3c treatments is probably a consequence of the ¹⁵N-enrichment during ongoing NO₃⁻ reduction of the added NO₃⁻ ²⁵. From day 4 onwards the $\delta^{15}\text{N}^{\text{bulk}}$ -N₂O values increased in the 1c treatment, indicating enrichment in ¹⁵N from a different pool of NO₃⁻. The ¹⁵N-enrichment of N₂O in the ¹⁵N-labelled 3c treatment showed that some of the N₂O (30 to 50%) came from soil-derived NO₃⁻. This suggests that pool 1 dominated initially (while the unlabelled treatment showed an increase in $\delta^{15}\text{N}^{\text{bulk}}$ -N₂O values) whereas, when the relative contribution of soil-NO₃⁻ increased (which can be seen by lowering of N₂O emission from fertiliser), the $\delta^{15}\text{N}^{\text{bulk}}$ values did not increase further, due to the increasing contribution from pool 2 masking any increases in $\delta^{15}\text{N}^{\text{bulk}}$ values from pool 1. In the 1c treatment, however, changes in the ¹⁵N-enrichment of the N₂O could be related to the influence of two N-pools; one core receiving amendment (soil N + added N) and two cores with only soil N with different denitrification dynamics where the fraction of N₂O varied over time. The observed dynamics are in line with earlier observations during incubation of NO₃⁻/glucose-amended soil cores ^{25,26} where the initial increase in $\delta^{15}\text{N}^{\text{bulk}}$ -N₂O values had been explained by the fast exhaustion of NO₃⁻ and the consequential ¹⁵N-enrichment of residual NO₃⁻ from pool 1 during the earlier phase, followed by declining N₂O fluxes from pool 1 after its exhaustion. The lowering of $\delta^{15}\text{N}^{\text{bulk}}$ values was explained as being from the growing contribution of pool 2 to N₂O fluxes, since pool 2 was previously less fractionated than pool 1 due to its lower denitrification rate in the absence of glucose. The final increase in $\delta^{15}\text{N}^{\text{bulk}}$ values was explained by N₂O fluxes from pool 2 since its NO₃⁻ was also progressively reduced and thus fractionated. The latter was verified by modelling of the $\delta^{15}\text{N}$ -N₂O values and it is further discussed in the isotopocules model section.

The ¹⁵N site preference

The SP of the N₂O is the result of several mechanisms responsible for N₂O production such as nitrification, bacterial and fungal denitrification ^{15,41-43}. The range of SP values in this study is in agreement with those from previous studies under denitrifying conditions ^{18,25,44}. Moreover, it is known that reduction of N₂O to N₂ causes ¹⁵N accumulation on the central N-position of the N₂O because of the cleavage of NO-bonds during this process ^{15,41}. In fact, we observed a N₂ peak after 5 days, in both the 1c and the 3c treatments, with higher SP values indicating the reduction of N₂O to N₂.

In this study, the decrease in ¹⁵N SP values of N₂O before the N₂O peak followed by an increase suggests that the site-specific ¹⁵N fractionation factor of the reduction of NO₃⁻ to N₂O was not constant in the 1c and 3c treatments. At the end of the experiment, the maximum SP value was reached, coinciding with minimum fluxes of N₂O and the lowest N₂O/(N₂+N₂O) ratio, suggesting an increase extent of the N₂O reduction ²⁵. Regardless of the amounts of N and total area amended, the variation of the SP N₂O between treatments was relatively small. This agrees with earlier studies ^{12,25,44} that explained the decline in SP values as resulting from the initiation of anaerobic conditions after inducing this process by flushing

with N₂ or with a decreasing contribution from fungal denitrification. It is possible that some N₂O emission resulted from nitrification although the soil moisture was adjusted to favour denitrification⁷.

The $\delta^{18}\text{O}$ signatures

The values of $\delta^{18}\text{O-N}_2\text{O}$ are determined by NO_3^- , O₂ and soil H₂O incorporation and reduction effects during the production of N₂O resulting in ¹⁸O-depleted or -enriched N₂O, respectively, since the ¹⁸O–N-bond is more stable and ¹⁶O is removed more easily from NO_3^- ^{42,44}. It is known that oxygen can be incorporated from H₂O to N₂O during denitrification to constitute more than 60% of the O in the N₂O produced^{45,46}. During the first four days of the incubation, the $\delta^{18}\text{O-N}_2\text{O}$ values increased indicating an independence of the $\delta^{18}\text{O-N}_2\text{O}$ values from the $\delta^{18}\text{O-NO}_3^-$ values during the production of N₂O that can be attributed to a lower O-exchange with water¹². Our results are in agreement with those reported by Meijide et al⁴⁴ and Bergstermann et al²⁵ showing stabilization of $\delta^{18}\text{O-N}_2\text{O}$ values after the N₂O peak. However, in contrast to Meijide et al⁴⁴ we did not observe an increase in $\delta^{18}\text{O-N}_2\text{O}$ values linked to an increase of N₂ fluxes.

In this study, different patterns of $\delta^{15}\text{N}^{\text{bulk}}$ vs $\delta^{18}\text{O}$ values (Figure 4 showing two clusters before and after the N₂O peak as well as differently sloped lines for the different treatments) suggested the temporal change in denitrification between the different pools before and after the N₂O peak. Before the N₂O peak, N₂O originated from non-fractionated NO_3^- in pool 1 (NO_3^- added from fertiliser) whereas after the N₂O peak the main flux might have come from pool 2 (mixture from fertiliser and native NO_3^-), which also contained less fractionated NO_3^- initially⁴⁴. Moreover, the patterns of SP vs $\delta^{18}\text{O}$ values gave further indications on processes contributing to N₂O fluxes^{18,47}: pre-peak values cluster mainly in the bacterial endmember area indicating little contribution from other sources and minor reduction in agreement with flux data, whereas post-peak values (>day 4) cluster around the reduction line, indicating bacterial production with varying reduction to N₂, where the latter is also confirmed by flux data (Figure 3). Interestingly, the peak values form a distinct cluster below the reduction line with SP values below zero per mil, indicative of bacterial production with minor reduction, but the $\delta^{18}\text{O}$ values are increased by 15 to 20‰ compared with the pre-flux values. Those data can thus not be explained with the “mapping approach” suggested by Lewicka-Szczebak et al,¹⁸ which assumes that the $\delta^{18}\text{O}$ value of bacterial N₂O prior to its reduction is relatively constant due to almost complete O-exchange with water, implying that a positive shift in the $\delta^{18}\text{O}$ value must be due to N₂O reduction and associated with increasing SP values. Because the $\delta^{15}\text{N}_{\text{bulk}}$ values exhibited a similar upshift until day 4, we assume that this effect is due to an increase in the $\delta^{18}\text{O}$ and $\delta^{15}\text{N}$ values of the NO_3^- precursor resulting from fractionation during intense denitrification in this phase of the experiment (day 4). This would also mean, however, that O-exchange with water during N₂O production was incomplete, which has been reported earlier for a dynamic incubation similar to our study⁴⁶.

Isotopocules model

The Rayleigh model^{25,26} was applied to account for the importance of N₂O emissions from the 1-pool and 2-pools using the $\delta^{15}\text{N}^{\text{bulk}}$ -values of N₂O. Until now, this model has been used to simulate the $\delta^{15}\text{N}$ values of N₂O using process rates and associated fractionation factors, but assumptions had to be made for some of the model parameters due to lack of available data²⁵. In this study, we carried out two incubation experiments in order to parameterise the model. The range of $\delta^{15}\text{N}^{\text{bulk}}$ values agrees with other studies that identified denitrification as the main N₂O producing process under similar conditions⁴⁴. Data from ¹⁵N-labelling showed an initial increase in the contribution of pool 1 followed by a decrease (Figure 3), which was sooner and larger in the 1c treatment. The comparison of the previously used Rayleigh model^{25,26} and the Rayleigh model adapted in this study according to $\delta^{15}\text{N}^{\text{bulk}}$ analysis of N₂O showed that a 2-pool model was better for interpreting the 1c treatment, whereas for the 3c treatment little difference between the modelling approaches was observed. This supports the idea that the amendment was mixed with parts of the soil pool, forming one uniform pool initially dominating N₂O emissions in treatment 3c. In this treatment the $\delta^{15}\text{N}^{\text{bulk}}$ levels stabilise after day 6, which indicates that a second pool contributes to emissions. Previous studies^{25,26} assumed that during the N₂O emission peak, a small but increasing contribution of pool 2 also occurs and its contribution was fitted assuming an exponential increase of pool 2 emission until reaching the emission observed after the extinction of pool 1. Using two different amendment areas, we found that a third order polynomial equation based on empirical $\delta^{15}\text{N}^{\text{bulk}}$ data improved the fit of the model, especially for the 1c treatment. Although we intended to control the magnitude of pool 1 (33% or 100% of amendment area) in this study, the Rayleigh model fit adapted to the ¹⁵N-labelling data showed a good third order polynomial fit for only two vessels per treatment. Thus, a better parameterising of the model should be addressed for examination of fractionation factors for various product ratios and reaction rates of pool 2 by future studies.

Conclusions

Determining N₂O emissions from different N-pools in soil is important for the interpretation of N₂O isotopocule data. This study shows the potential for understanding the source of N₂O emissions from different N pools using an improved model for the interpretation of N₂O isotopocule data. It was indicated that the assumptions regarding the exponential increase of pool 2 activity accepted in previous studies^{25,26} should be replaced with a polynomial increase with dependence on both pools sizes. Our results show the value of parameterising models under controlled laboratory conditions using experimental data but further work is required to apply the findings to other soil types and improve the refinement of model parameters.

Acknowledgements

Rothamsted Research receives strategic funding by the Biotechnology and Biological Sciences Research Council (BBSRC). This study was funded by BBSRC project BB/K001051/1. D.

References

1. IPCC. Climate change. In: *Synthesis report of the fourth assessment report of IPCC, chapter 2.10.2*. 2007.
2. Crutzen PJ, Atmospheric chemical processes of the oxides of nitrogen, including nitrous oxide, In: Delwiche CC, ed. *Denitrification, nitrification, and atmospheric nitrous oxide*. New York, N.Y: John Wiley & Sons Inc.; 1981:17-44.
3. Cárdenas LM, Hawkins JMB, Chadwick D, Scholefield D. Biogenic gas emissions from soils measured using a new automated laboratory incubation system. *Soil Biol Biochem*. 2003;35(6):867-870.
4. Scholefield D, Hawkins JMB, Jackson SM. Development of a helium atmosphere soil incubation technique for direct measurement of nitrous oxide and dinitrogen fluxes during denitrification. *Soil Biol Biochem*. 1997;29(9–10):1345-1352.
5. Scholefield D, Hawkins JMB, Jackson SM. Use of a flowing helium atmosphere incubation technique to measure the effects of denitrification controls applied to intact cores of a clay soil. *Soil Biol Biochem*. 1997;29(9–10):1337-1344.
6. Baggs EM. A review of stable isotope techniques for N₂O source partitioning in soils: recent progress, remaining challenges and future considerations. *Rapid Commun Mass Spectrom*. 2008;22(11):1664-1672.
7. Well R, Flessa H, Lu X, Ju X, Romheld V. Isotopologue ratios of N₂O emitted from microcosms with NH₄⁺ fertilized arable soils under conditions favoring nitrification. *Soil Biol Biochem*. 2008;40(9):2416-2426.
8. Yamulki S, Toyoda S, Yoshida N, Veldkamp E, Grant B, Bol R. Diurnal fluxes and the isotopomer ratios of N₂O in a temperate grassland following urine amendment. *Rapid Commun Mass Spectrom*. 2001;15(15):1263-1269.
9. Bol R, Toyoda S, Yamulki S, Hawkins JMB, Cardenas LM, Yoshida N. Dual isotope and isotopomer ratios of N₂O emitted from a temperate grassland soil after fertiliser application. *Rapid Commun Mass Spectrom*. 2003;17(22):2550-2556.
10. Cardenas LM, Chadwick D, Scholefield D, et al. The effect of diet manipulation on nitrous oxide and methane emissions from manure application to incubated grassland soils. *Atmos Environ*. 2007;41(33):7096-7107.
11. Pérez T, Garcia-Montiel D, Trumbore S, et al. Nitrous oxide nitrification and denitrification 15N enrichment factors from Amazon forest soils. *Ecol Appl*. 2006;16(6):2153-2167.
12. Well R, Flessa H. Isotopologue signatures of N₂O produced by denitrification in soils. *Journal of Geophysical Research: Biogeosciences*. 2009;114(G2):G02020.
13. Yoshida N. 15N-depleted N₂O as a product of nitrification. *Nature*. 1988;335:528-529.
14. Menyailo OV, Hungate BA. Stable isotope discrimination during soil denitrification: Production and consumption of nitrous oxide. *Global Biogeochem Cycles*. 2006;20(3):GB3025.
15. Ostrom NE, Pitt A, Sutka R, et al. Isotopologue effects during N₂O reduction in soils and in pure cultures of denitrifiers. *Journal of Geophysical Research: Biogeosciences*. 2007;112(G2):G02005.
16. Jinuntuya-Nortman M, Sutka RL, Ostrom PH, Gandhi H, Ostrom NE. Isotopologue fractionation during microbial reduction of N₂O within soil mesocosms as a function of water-filled pore space. *Soil Biol Biochem*. 2008;40(9):2273-2280.
17. Toyoda S, Mutoke H, Yamagishi H, Yoshida N, Tanji Y. Fractionation of N₂O isotopomers during production by denitrifier. *Soil Biol Biochem*. 2005;37(8):1535-1545.
18. Lewicka-Szczebak D, Augustin J, Giesemann A, Well R. Quantifying N₂O reduction to N₂ based on N₂O isotopocules - validation with independent methods (helium incubation and 15N gas flux method). *Biogeosciences*. 2017;14:711-732.
19. Toyoda S, Yoshida N. Determination of Nitrogen Isotopomers of Nitrous Oxide on a Modified Isotope Ratio Mass Spectrometer. *Anal Chem*. 1999;71(20):4711-4718.

20. Brenninkmeijer CAM, Röckmann T. Mass spectrometry of the intramolecular nitrogen isotope distribution of environmental nitrous oxide using fragment-ion analysis. *Rapid Commun Mass Spectrom.* 1999;13(20):2028-2033.
21. Popp BN, Westley MB, Toyoda S, et al. Nitrogen and oxygen isotopomeric constraints on the origins and sea-to-air flux of N₂O in the oligotrophic subtropical North Pacific gyre. *Global Biogeochemical Cycles.* 2002;16(4):12-11-12-10.
22. Sutka RL, Adams GC, Ostrom NE, Ostrom PH. Isotopologue fractionation during N₂O production by fungal denitrification. *Rapid Commun Mass Spectrom.* 2008;22(24):3989-3996.
23. Wu D, Koster JR, Cardenas LM, Bruggemann N, Lewicka-Szczebak D, Bol R. N₂O source partitioning in soils using (15)N site preference values corrected for the N₂O reduction effect. *Rapid Commun Mass Spectrom.* 2016;30(5):620-626.
24. Groffman PM, Butterbach-Bahl K, Fulweiler RW, et al. Challenges to incorporating spatially and temporally explicit phenomena (hotspots and hot moments) in denitrification models. *Biogeochemistry.* 2009;93(1):49-77.
25. Bergstermann A, Cárdenas L, Bol R, et al. Effect of antecedent soil moisture conditions on emissions and isotopologue distribution of N₂O during denitrification. *Soil Biol Biochem.* 2011;43(2):240-250.
26. Lewicka-Szczebak D, Well R, Bol R, et al. Isotope fractionation factors controlling isotopocule signatures of soil-emitted N₂O produced by denitrification processes of various rates. *Rapid Commun Mass Spectrom.* 2015;29(3):269-282.
27. Loick N, Dixon E, Abalos D, et al. "Hot spots" of N and C impact nitric oxide, nitrous oxide and nitrogen gas emissions from a UK grassland soil. *Geoderma.* 2017;305:336-345.
28. Denk TRA, Mohn J, Decock C, et al. The nitrogen cycle: a review of isotope effects and isotope modeling approaches. *Soil Biol Biochem.* 2017;105:121-137.
29. Mariotti A, Germon JC, Hubert P, et al. Experimental determination of nitrogen kinetic isotope fractionation: Some principles; illustration for the denitrification and nitrification processes. *Plant Soil.* 1981;62(3):413-430.
30. Cardenas LM, Bol R, Lewicka-Szczebak D, et al. Effect of soil saturation on denitrification in a grassland soil. *Biogeosci Disc.* 2017;14:4691-4710.
31. Kieft TL, Soroker E, Firestone MK. Microbial biomass response to a rapid increase in water potential when dry soil is wetted. *Soil Biol Biochem.* 1987;19(2):119-126.
32. Morecroft MD, Bealey CE, Beaumont DA, et al. The UK Environmental Change Network: Emerging trends in the composition of plant and animal communities and the physical environment. *Biol Conserv.* 2009;142(12):2814-2832.
33. RoTAP. *Review of Transboundary Air Pollution: Acidification, Eutrophication, Ground Level Ozone and Heavy Metals in the UK.* Contract Report to the Department for Environment, Food and Rural Affairs. Centre for Ecology & Hydrology. 2012.
34. Laughlin RJ, Stevens RJ, Zhuo S. Determining Nitrogen-15 in Ammonium by Producing Nitrous Oxide. *Soil Sci Soc Am J.* 1997;61(2):462-465.
35. Searle PL. The Berthelot or indophenol reaction and its use in the analytical chemistry of nitrogen. A review. *Analyst.* 1984;109:549-568.
36. Tiedje JM, Ecology of denitrification and dissimilatory nitrate reduction to ammonium, In: Zehnder AJB, ed. *Biology of Anaerobic Microorganisms.* New York, USA: John Wiley & Sons; 1988:179-244.
37. Wang R, Feng Q, Liao T, et al. Effects of nitrate concentration on the denitrification potential of a calcic cambisol and its fractions of N₂, N₂O and NO. *Plant Soil.* 2013;363(1-2):175-189.
38. Saggarr S, Jha N, Deslippe J, et al. Denitrification and N₂O:N₂ production in temperate grasslands: Processes, measurements, modelling and mitigating negative impacts. *Sci Total Environ.* 2013;465(0):173-195.

39. Jones CM, Stres B, Rosenquist M, Hallin S. Phylogenetic analysis of nitrite, nitric oxide, and nitrous oxide respiratory enzymes reveal a complex evolutionary history for denitrification. *Mol Biol Evol.* 2008;25(9):1955-1966.
40. Loick N, Dixon ER, Abalos D, et al. Denitrification as a source of nitric oxide emissions from incubated soil cores from a UK grassland soil. *Soil Biol Biochem.* 2016;95:1-7.
41. Schmidt HL, Werner RA, Yoshida N, Well R. Is the isotopic composition of nitrous oxide an indicator for its origin from nitrification or denitrification? A theoretical approach from referred data and microbiological and enzyme kinetic aspects. *Rapid Commun Mass Spectrom.* 2004;18(18):2036-2040.
42. Well R, Kurganova I, Lopes de Gerenyu V, Flessa H. Isotopomer signatures of soil emitted N₂O under different moisture conditions - a microcosm study with arable loess soil. *Soil Biol Biochem.* 2006;38(9):2923-2933.
43. Röhe L, Well R, Lewicka-Szczebak D. Use of oxygen isotopes to differentiate between nitrous oxide produced by fungi or bacteria during denitrification. *Rapid Commun Mass Spectrom.* 2017;31(16):1297-1312.
44. Meijide A, Cardenas LM, Bol R, et al. Dual isotope and isotopomer measurements for the understanding of N₂O production and consumption during denitrification in an arable soil. *Eur J Soil Sci.* 2010;61(3):364-374.
45. Casciotti KL, Sigman DM, Hastings MG, Bohlke JK, Hilkert A. Measurement of the oxygen isotopic composition of nitrate in seawater and freshwater using the denitrifier method. *Anal Chem.* 2002;74(19):4905-4912.
46. Lewicka-Szczebak D, Dyckmans J, Kaiser J, Marca A, Augustin J, Well R. Oxygen isotope fractionation during N₂O production by soil denitrification. *Biogeosciences.* 2016;13:1129-1144.
47. Buchen C, Lewicka-Szczebak D, Flessa H, Well R. Estimating N₂O processes during grassland renewal and grassland conversion to maize cropping using N₂O isotopocules. *Rapid Commun Mass Spectrom.* 2018;32(13):1053-1067.

Tables

Table 1. Soil characteristics at the end of the experiment. Total amounts measured for nitrate (NO_3^-) and ammonium (NH_4^+). '1c' = average values for 12 cores (4 amended with 75 kg N ha^{-1} , 8 unamended) from vessels of treatment 1c; '3c' = average values for 12 cores (12 amended with 75 kg N ha^{-1}) of treatment 3c; 'Control' = average of 12 cores from the Control treatment only receiving water. Different letters indicate a significant difference between treatments for each layer (Top or Bottom); * indicates significant difference between the top and bottom layer within a single grouping. (n=10 for '1c' and '3c', n=4 for 'Control'), $p < 0.05$). Standard errors are included. NO_3^- -N (mg g^{-1} dry soil) values were $4.6 \cdot 10^{-2} \pm 2.0 \cdot 10^{-4}$ and $9.8 \cdot 10^{-3} \pm 4.0 \cdot 10^{-4}$ before and after priming, respectively, before amendment application. NH_4^+ -N (mg g^{-1} dry soil) amount was $6.0 \cdot 10^{-3} \pm 9.0 \cdot 10^{-6}$ before amendment application.

Parameter	Layer	1c	3c	Control
NO_3^- (mg N g^{-1} dry soil)	Top	$1.44 \pm 0.06^{\text{B}*}$	$1.68 \pm 0.05^{\text{A}*}$	$1.23 \pm 0.13^{\text{B}}$
	Bottom	$1.28 \pm 0.04^{\text{A}*}$	$1.36 \pm 0.04^{\text{A}*}$	$1.13 \pm 0.03^{\text{B}}$
NH_4^+ (mg N g^{-1} dry soil)	Top	$0.055 \pm 0.002^{\text{B}*}$	$0.050 \pm 0.001^{\text{C}*}$	$0.060 \pm 0.001^{\text{A}*}$
	Bottom	$0.069 \pm 0.004^{\text{A}*}$	$0.066 \pm 0.003^{\text{A}*}$	$0.076 \pm 0.005^{\text{A}*}$
WFPS (%)	Top		$83.2 \pm 0.50^*$	
	Bottom		$76.0 \pm 0.56^*$	

Table 2. Cumulative emissions of NO, N₂O, N₂ as kg N ha⁻¹ and CO₂ as kg C ha⁻¹. Values were determined in the period between the start and end of the emission peak: NO day 0-4, N₂O day 0-10, N₂ day 4.5 to 9.5, CO₂ day 0-10 after amendment application. Different letters indicate a significant difference between treatments for each measured gas (n=8 for 1c and 3C, n=4 for Control; p <0.05). Standard errors of the mean are included.

Gas	1c	3C	Control
NO	0.0079 ± 0.0005 ^B	0.0183 ± 0.0021 ^A	0.0018 ± 0.0003 ^C
N ₂ O	6.73 ± 1.37 ^B	19.49 ± 5.04 ^A	1.14 ± 0.13 ^C
N ₂	2.88 ± 0.56 ^B	5.91 ± 2.25 ^A	3.02 ± 0.93 ^B
CO ₂	192.23 ± 3.65 ^B	313.66 ± 10.07 ^A	122.41 ± 6.73 ^C
Total N	9.46 ± 1.01 ^B	26.12 ± 6.59 ^A	4.28 ± 0.89 ^B

Accepted Article

Table 3. Measured isotopic ratios of emitted N₂O, as $\delta^{18}\text{O}$, $\delta^{15}\text{N}^{\text{bulk}}$ and Site Preference (SP) in those 1c and 3c treatments that received unlabelled KNO₃ with their amendment as well as the Control treatment over the time of the incubation.

Days after treatment	$\delta^{18}\text{O}$ values (‰)			$\delta^{15}\text{N}^{\text{bulk}}$ values (‰)			SP (‰)		
	1c	3c	Control	1c	3c	Control	1c	3c	Control
0	25.6	24.0	39.7	-23.4	-23.3	-23.8	-1.6	-4.9	22.4
2	21.4	21.7	18.9	-18.0	-16.9	-26.0	-6.0	-5.7	-4.1
4	37.3	38.9	30.1	-1.1	-5.5	-8.1	-6.3	-5.5	-3.7
6	43.3	41.7	31.1	10.4	-1.2	10.4	3.6	1.8	3.9
9	39.6	42.4	31.9	-4.2	1.0	-19.8	7.0	3.1	6.4
11	42.1	42.1	37.9	51.8	1.7	-20.7	9.4	4.3	22.9

Accepted Article

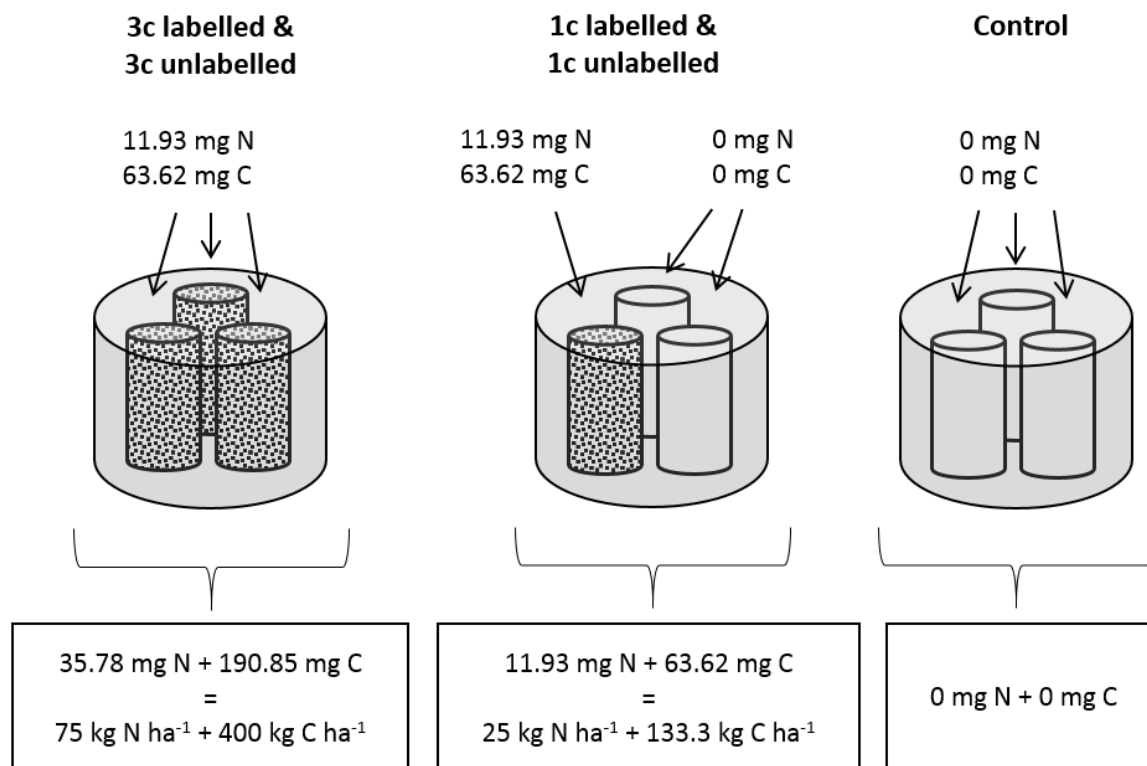


Figure 1. Schematic showing the N and C application rates and amounts of added N and C with the different treatments. Top values are amounts of N and C in mg added per core; Bottom values are amounts of N and C in mg added to the whole vessel and the rate this equates to in kg ha⁻¹ per vessel: 3c = nutrients applied to all three cores; 1c = nutrients applied to one core; Control = no nutrient application to any core. Each small core contained 95.3 g dry soil.

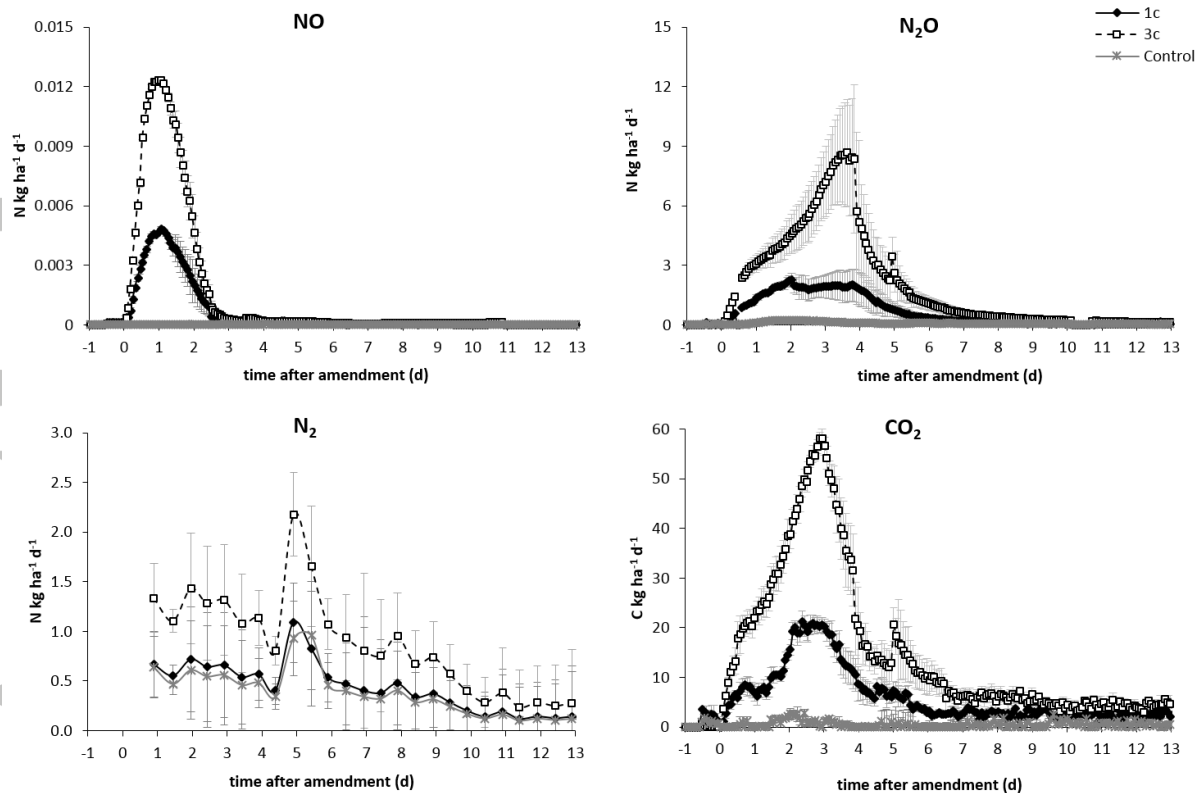


Figure 2. Average fluxes of NO, N₂O, N₂ and CO₂ for the different treatments (n =8). In treatment 1c one of the three cores inside a vessel was amended with KNO₃ and glucose (the other two received water); in the 3c, all three of the cores inside a vessel were amended with KNO₃ and glucose (each core received the same N and C rate as the 1c treatment); in the Control, only water was applied to each of the three cores.

Accepted

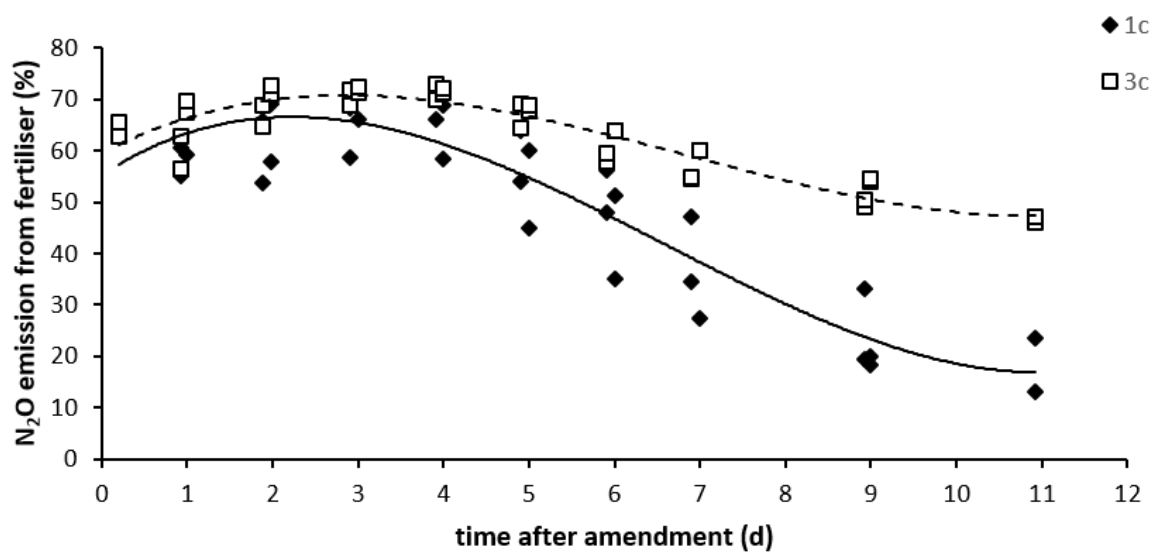


Figure 3. Contribution of fertiliser applied N to N₂O emissions as determined from ¹⁵N enrichment of the emitted N₂O from those 1c and 3c treatments that had received ¹⁵N-labelled KNO₃ with their amendment.

Accepted

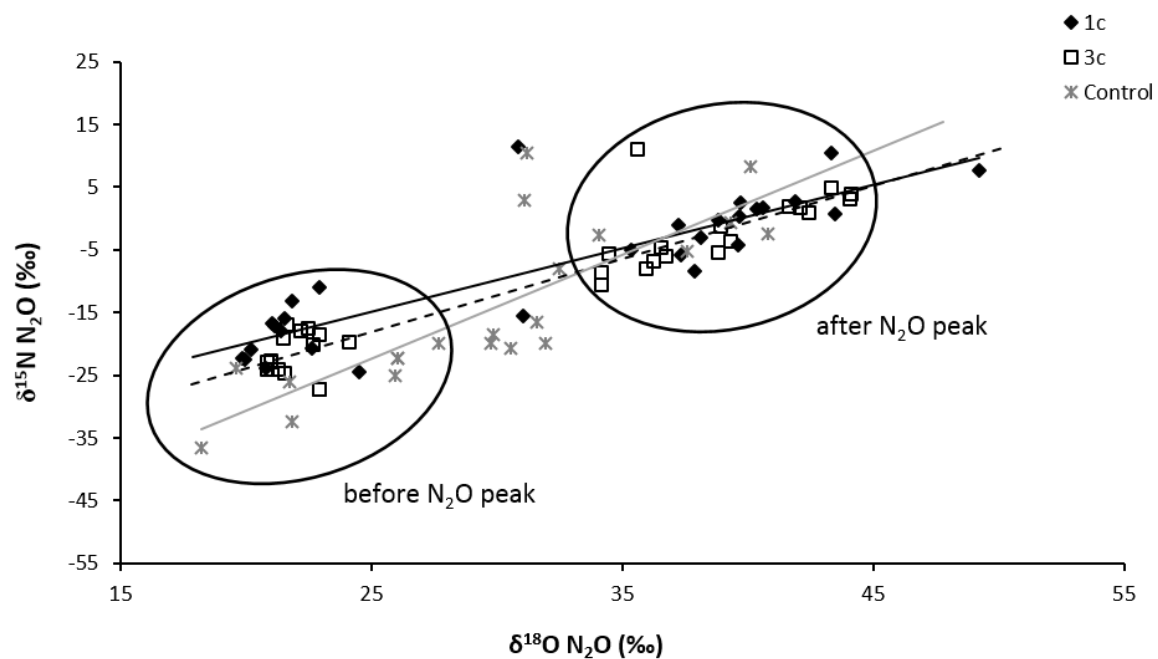


Figure 4. Comparison of $\delta^{15}\text{N}$ bulk and $\delta^{18}\text{O}$ values of soil emitted N_2O from those 1c and 3c treatments that had received unlabelled KNO_3 with their amendment as well as the Control treatment.

Accepted

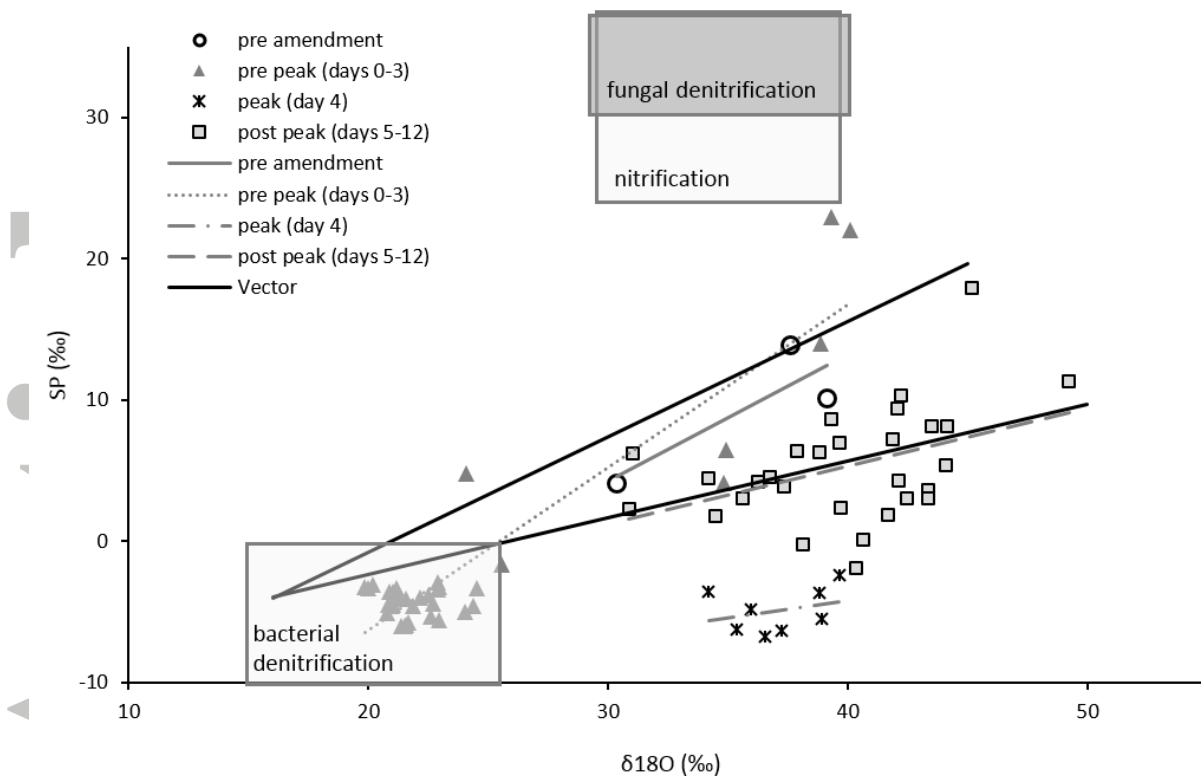


Figure 5. SP vs $\delta^{18}\text{O}$ values from all vessels that had received unlabelled amendment, grouped for four time periods depending on the appearance of the peak in N_2O emissions (circle=pre amendment; triangle = after amendment application, but before the N_2O peak (days 0-3); cross = during the N_2O peak (day 4); square = post N_2O peak (days 5-12), all with associated trendlines (see legend)). The solid black lines are reduction lines after Lewicka-Szczebak et al. ¹⁸ representing minimum and maximum routs of isotopocule values with increasing N_2O reduction to N_2 . Endmember areas for fungal denitrification, nitrification and bacterial denitrification are from Lewicka-Szczebak et al. ¹⁸.

Accepted Article

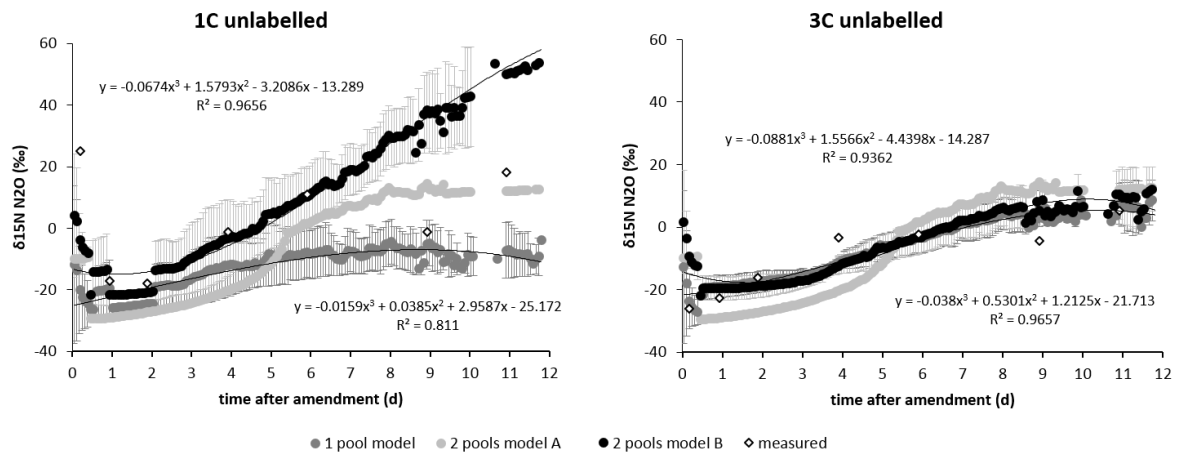


Figure 6. Comparison of modelled and measured data for the previously used Rayleigh model (model A) and the Rayleigh model adapted according to ^{15}N data (model B) for the two treatments 1c (left) and 3c (right) assuming 1-pool emission (only from fertiliser) and 2-pool emission (from fertiliser and soil nitrate). Equations relate to the adapted 2-pool model B (top equation) and the 1-pool model (bottom equation).

Accepted Article